Current Biology 18, 152–157, January 22, 2008 ©2008 Elsevier Ltd All rights reserved DOI 10.1016/j.cub.2007.12.056

Report

Minus-End-Directed Motor Ncd Exhibits Processive Movement that Is Enhanced by Microtubule Bundling In Vitro

Ken'ya Furuta[1] and Yoko Yano Toyoshima[1,*]
[1]Department of Life Sciences
Graduate School of Arts and Sciences
The University of Tokyo
Komaba 3-8-1, Meguro-ku
Tokyo, 153-8902
Japan

Summary

Drosophila **Ncd, a kinesin-14A family member, is essential for meiosis and mitosis [1–7]. Ncd is a minus-end-directed motor protein that has an ATP-independent microtubule binding site in the tail region, which enables it to act as a dynamic crosslinker of microtubules to assemble and maintain the spindle [8–12]. Although a tailless Ncd has been shown to be nonprocessive [13–16], the role of the Ncd tail in single-molecule motility is unknown. Here, we show that individual Ncd dimers containing the tail region can move processively along microtubules at very low ionic strength, which provides the first evidence of processivity for minus-end-directed kinesins. The movement of GFP-Ncd consists of both a unidirectional and a diffusive element, and it was sensitive to ionic strength. Motility of a truncation series of Ncd and removal of the tubulin tail suggested that the Ncd tail serves as an electrostatic tether to microtubules. Under higher ionic conditions, Ncd showed only a small bias in diffusion along "single" microtubules, whereas it exhibited processive movement along "bundled" microtubules. This property may allow Ncd to accumulate preferentially in the vicinity of focused microtubules and then to crosslink and slide microtubules, possibly contributing to dynamic spindle self-organization.**

Results and Discussion

Oligomeric State of the GFP-Ncd Proteins

To examine the motility of Ncd, we generated an N-terminal truncation series of Ncd fused with GFP (Figure 1A and Figure S1 available online). We first estimated the oligomeric state of all proteins. Sucrose density gradient centrifugation and gel-filtration analysis showed that GFP-Ncd320 and longer constructs form stable dimers in solution, whereas GFP-Ncd333 forms a monomer (Table S1). We further evaluated the oligomeric state of GFP-Ncd26 and GFP-Ncd195 by measuring the fluorescence intensities of GFP spots with a total internal reflection fluorescence (TIRF) microscope (Figure S4). The fluorescence intensities indicate that these spots correspond to single molecules of Ncd dimer even on the MT, where local motor-protein density could be high.

GFP-Ncd Constructs Containing the N-Terminal Tail Region Exhibit Processive Movement

The behavior of single molecules of GFP fusion proteins was tested in a motility assay by using a TIRF microscope at an ionic strength of 5 mM potassium acetate (KAc) in the presence of ATP. A nearly full-length construct, GFP-Ncd26, showed processive motility on microtubules (MTs) (Figures 1B and 1C and Movie S1). Moreover, GFP-Ncd195, which contains the whole stalk domain but lacks the tail domain, also showed processive motility, whereas GFP-Ncd222 and shorter constructs did not (Figure 1D). Although the movement of GFP-Ncd26 and GFP-Ncd195 was primarily unidirectional, there were occasional pauses and brief backward movements (Figure 1C). To quantify the bias of the movements, we calculated the instantaneous velocity from the pairwise distance (Figure 1E and Table 1) [17]. We found that GFP-Ncd26 and GFP-Ncd195 had clear directionality, but GFP-Ncd222 and GFP-Ncd236 only had a small or no bias toward the minus end of MTs (p values for the hypothesis that the mean equals zero were 0.74 and 0.0022 for GFP-Ncd222 and GFP-Ncd236, respectively; Student's t test). For GFP-Ncd26, approximately half of the molecules did not move but remained attached to MTs, probably via the ATP-independent MT binding site in the N-terminal tail domain (amino acid residues 83–100 and 115–187) [9], whereas shorter constructs rarely showed such behavior. Thus, for GFP-Ncd26, we classified all runs into moving and nonmoving fractions (see Supplemental Experimental Procedures). The classification seemed to work well: 41% of all tracked runs were excluded, but a considerable population remained with near-zero velocity. This population may reflect that GFP-Ncd26 paused during processive movement, which would lead to an underestimation of the velocity. We next quantified the diffusive element by plotting the mean square displacement (MSD) versus time interval [18] (Figure 1G). The quadratic fit $[\rho(\tau) = 2D\tau + v^2\tau^2 + C]$ to MSD plots of GFP-Ncd26 and GFP-Ncd195 gave a diffusion coefficient D that was larger than that of kinesin-GFP and larger than expected for a Poisson stepper with a step size of 8 nm and a mean velocity of 100 nm/s ($D = \sim 1000\ nm^2/s$) [19]. The values are rather consistent with the movement that can be described as a biased Brownian motion along MTs, as previously discussed [18, 20]. The fit also gave a drift velocity v (GFP-Ncd26: -47 ± 22 nm/s; GFP-Ncd195: -91 ± 46 nm/s), consistent with the instantaneous velocity. Mean duration and run length were decreased by N-terminal truncation (Table 1, Figure 1F, and Figure S3): The most marked difference was between the processive motility of GFP-Ncd195 and the nonprocessive motility of GFP-Ncd222, though both proteins had similar velocity in multiple-molecule MT-gliding assays. Thus, we will hereafter focus on GFP-Ncd195 and GFP-Ncd222 to identify the exact factor that ensures processive movement.

The Movement of GFP-Ncd195 Is Supported by Electrostatic Interactions

We predicted that the processive movement is supported by weak electrostatic interactions between GFP-Ncd195 and MTs. To test this idea, we observed the movement of GFP-Ncd195 in varying salt concentrations (Figure 2A). At 55 mM KAc or higher ionic strengths, the movement of GFP-Ncd195 was diffusive and had only a small bias toward the minus end of MTs ($p < 0.0001$, Student's t test), whereas

*Correspondence: cyytoyo@mail.ecc.u-tokyo.ac.jp

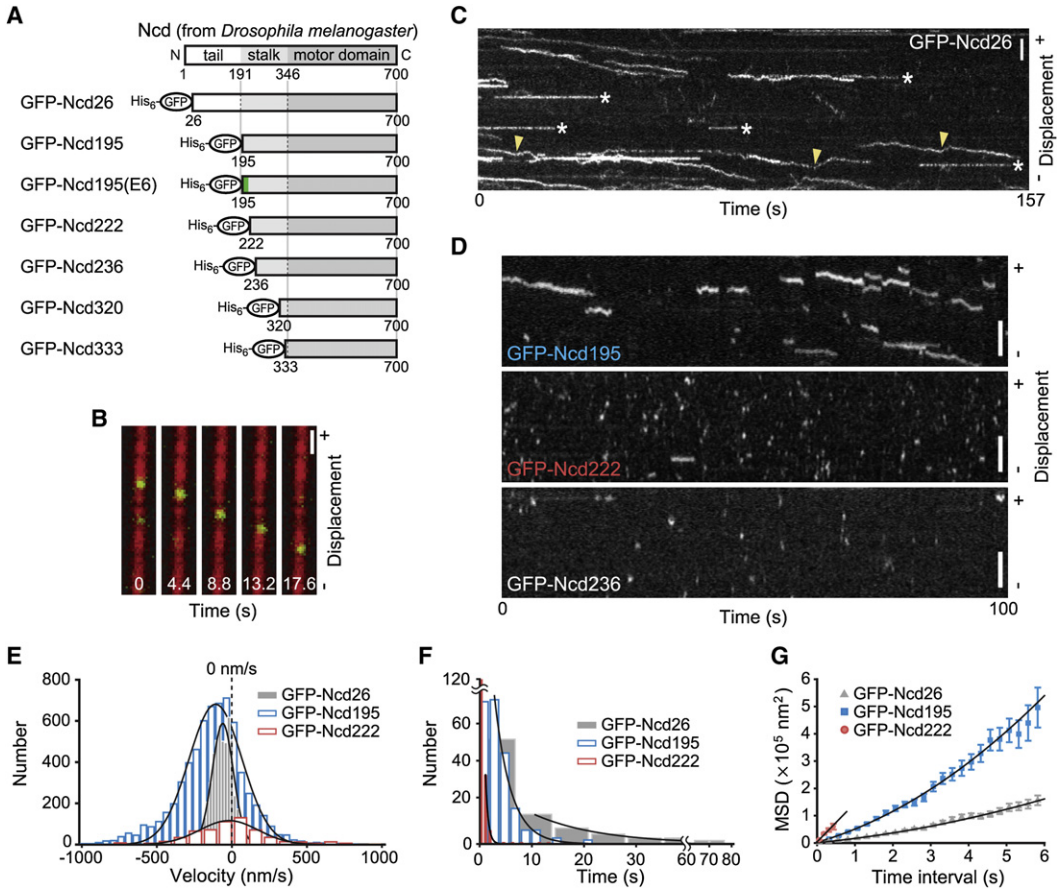

Figure 1. GFP-Ncd Movements along MTs

(A) Schematic representation of GFP-Ncd constructs. Full-length Ncd is shown at the top with the N-terminal basic tail domain (1–191), followed by the stalk domain (192–346, α-helical coiled coil), and the catalytic motor domain (347–700). GFP and a six-histidine tag were fused to the N terminus of all constructs. The green region at the N terminus of GFP-Ncd195(E6) represents the mutation in the K-rich region (see text).

(B) Sequential frames from a TIRF recording of GFP-Ncd26 movement. Five frames from a continuous GFP recording (green) were overlaid on one Cy5 image of the MT (red). Plus (+) and minus (−) symbols on the right refer to the polarity of the MT. Scale bar represents 1 μm.

(C) A kymograph showing the movement of GFP-Ncd26 along the MT in the presence of ATP. Arrowheads show examples of backward movements. Asterisks (*) denote typical nonmoving molecules. Scale bar represents 3 μm.

(D) Kymographs showing the movements of GFP-Ncd proteins along MTs. Scale bars represent 3 μm.

(E) Histograms of instantaneous velocities and durations of GFP-Ncd26, 195, and 222 with the fitted Gaussian curves. The dashed line represents the position of zero velocity.

(F) Histograms of durations of GFP-Ncd26, 195, and 222. The regressions were performed by using cumulative probability distribution to determine the mean durations (see Figure S3).

(G) MSD plots of GFP-Ncd26, 195, and 222 with the fitted quadratic curves. Each plot represents mean ± SEM.

kinesin-GFP showed processive motility at 105 mM KAc [21]. The high sensitivity of GFP-Ncd195 to ionic strength suggests that the movement of GFP-Ncd195 is supported by electrostatic interactions.

We further predicted that GFP-Ncd195 is tethered via the negatively charged C terminus of tubulin, known as the E-hook. To test this, we repeated the single-molecule motility assays using subtilisin-digested MTs that lack the E-hook (Figure S5). Figure 2B and Table 1 show that GFP-Ncd195 is unable to move processively along the digested MT. The loss of processivity could be due to structural defects in the digested MT, but the smooth movement of kinesin-GFP in our single-molecule motility assay and a recent structural study [22] do not support this notion. Hence, we conclude that loss of processivity on subtilisin-digested MTs is due to the absence of the E-hook, as previously discussed [23].

Considering the marked difference in processivity between GFP-Ncd195 and GFP-Ncd222, the N-terminal first quarter of the stalk domain (F195-G221) of Ncd195 is sufficient to convert the nonprocessive GFP-Ncd222 construct into a processive one. This region is highly basic, containing six lysines and one arginine in 20 amino acids (hereafter referred to as the "K-rich" region, Figure 2C). To test whether this region is the electrostatic partner of the E-hook, we produced a mutant construct, GFP-Ncd195(E6), in which six lysines in the K-rich region were replaced by glutamates. The velocity and run length of this mutant decreased to levels similar to wild-type on subtilisin-digested MTs (Figure 2B and Table 1), suggesting that these residues are responsible for the stability of the interaction with MTs. It is possible that the K-rich region forms a stable coiled-coil structure, as predicted by the amphipathy score [24], therefore we cannot completely rule out the

Table 1. Summary of Single-Molecule Motility Assays on Single MTs in the Presence of ATP

Construct	Oligomeric State	Velocity (nm/s)	Run Length (nm)	Duration (s)	Diffusion Coefficient ($\times 10^4$ nm^2/s)	n	MT Gliding Velocity (nm/s)
GFP-Ncd26	Dimer	−46 ± 2	−540 ± 57	8.8 ± 0.5	1.0 ± 0.1	151	150 ± 3
GFP-Ncd195	Dimer	−97 ± 4	−430 ± 40	3.4 ± 0.6	2.0 ± 0.3	230	135 ± 6
GFP-Ncd222	Dimer	−20 ± 11	−40 ± 24	0.57 ± 0.04	7.1 ± 3.1	207	136 ± 10
GFP-Ncd236	Dimer	−20 ± 13	−52 ± 16	0.77 ± 0.01	2.3 ± 0.6	219	112 ± 4
GFP-Ncd195(E6)	Dimer	−2.1 ± 0.9	−95 ± 16	2.2 ± 0.1	0.53 ± 0.11	205	138 ± 4
GFP-Ncd195 on dMT	Dimer	−1.5 ± 1.3	−15 ± 26	3.2 ± 0.1	0.69 ± 0.10	83	102 ± 6
GFP-Ncd195[a]	Dimer	−72 ± 2	−440 ± 10	4.6 ± 0.1	ND	107	ND
Kinesin-GFP	Dimer	690 ± 5	1620 ± 19	2.8 ± 0.1	0.48 ± 0.08	109	760 ± 16

Velocities were determined from Gaussian fits to the instantaneous velocities. The minus (−) symbol refers to the polarity of the MT. Errors are given as the standard error of the fitted parameter, except for the standard errors of run length of GFP-Ncd that were calculated from the raw data. n is the number of runs that were scored for each construct from 3–5 different flow chambers. MT gliding velocities were determined from 30–50 MTs. ND, not determined.

[a] Single-molecule motility assays were carried out on a negatively-charged glass surface. Although the coverslips were coated with casein to prevent nonspecific interactions, we wished to foreclose the possibility that GFP-Ncd195 can interact with the glass surface to move processively on MTs. We therefore observed the motility on a hydrophobic silanized surface. The movement was unidirectional and essentially comparable to that on a nonsilanized glass surface.

possibility that the mutation could break the coiled-coil structure of this region and cause the observed decrease in velocity and run length. However, this does not seem to be the case. It is unlikely that the K-rich region forms a stable coiled-coil structure for two reasons. First, the K-rich region (F195-G221) and the remaining C-terminal part (E222-R346) of the stalk domain belong to different types of heptad frames and have a proline residue at the boundary that could cause a kink in the structure (Figure S2). Second, the synthetic peptide fragment (K188-T275) containing the K-rich region (F195-G221) is unable to form a coiled coil [25]. Therefore, we consider that the positive charge in the K-rich region, not the coiled-coil structure, ensures processive movement by interacting with the negatively charged E-hook of tubulin.

The N-Terminal Tail Region Affects the MT-Activated ATPase Activity

We next examined the biochemical properties of GFP-Ncd195 and GFP-Ncd222 by measuring the MT-activated ATPase activity (Figure 2D). GFP-Ncd195 and GFP-Ncd222 had the same k_{cat} value of 1.6 s^{-1} but had different $K_{m,MT}$ values of 0.22 and 0.44 μM, respectively. When comparing GFP-Ncd195 with GFP-Ncd222, the decreased $K_{m,MT}$ of GFP-Ncd195 is qualitatively consistent with the longer duration observed in the motility assay, but not quantitatively consistent (two-fold and six-fold for the ATPase and motility assay, respectively). We suppose that the $K_{m,MT}$ values would not directly reflect the observed difference in duration for two possible reasons. First, Ncd molecules that move in short periods (up to about 200 ms) are ignored in the motility assay but are likely to substantially contribute to the ATPase rate. Second, the degradation products that contain the motor domain (Figure S1) might reduce the apparent difference in ATPase activity between the two constructs because these truncated products would have higher ATPase activity and affinity for MTs [26, 27]. Thus, although the difference in the ATPase assay was smaller than that observed in the motility assay, the result is consistent with the idea that the N-terminal region of Ncd195 enhances its affinity for MTs.

Dimeric Ncd Heads Can Diffuse along MTs in the Weak Binding State

We speculated that the diffusive element of the processive movement would not require ATP hydrolysis. To test this, we carried out motility assays of GFP-Ncd proteins in the presence of saturating ADP. Notably, GFP-Ncd320 (a dimer

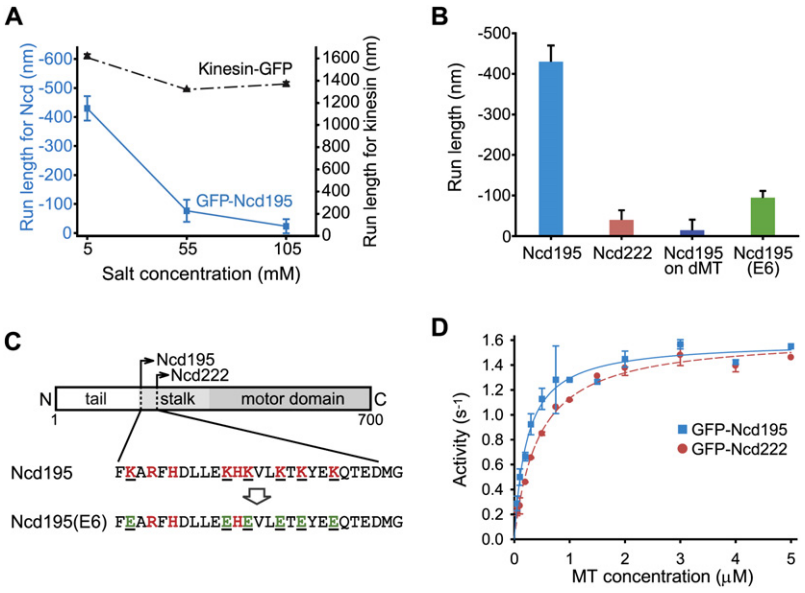

Figure 2. Effect of Electrostatic Interactions on the Motility and Biochemical Properties of GFP-Ncd Proteins

(A) Run lengths of kinesin-GFP and GFP-Ncd195 on single MTs as a function of salt concentration. Each plot represents the mean ± SEM. Note that the vertical scales are different for Ncd (blue) and kinesin (black).

(B) Effects of subtilisin digestion and mutation of the K-rich region on the run length of GFP-Ncd195. Each bar represents the mean ± SEM.

(C) Schematic representation of the K-rich region. The basic amino acid residues are shown in red, and the acidic residues introduced by mutagenesis are shown in green.

(D) Steady-state MT-activated ATPase activities of GFP-Ncd proteins. The ATPase activity is expressed per Ncd motor domain and the MT concentration expressed per tubulin heterodimer. Each plot represents the mean ± SD from two or three independent experiments. The plots show hyperbolic dependence with a same k_{cat} value of 1.6 ± 0.1 s^{-1} for the two constructs and different $K_{m,MT}$ values of 0.22 ± 0.04 μM and 0.44 ± 0.02 μM for GFP-Ncd195 (blue solid line) and GFP-Ncd222 (red dashed line), respectively.

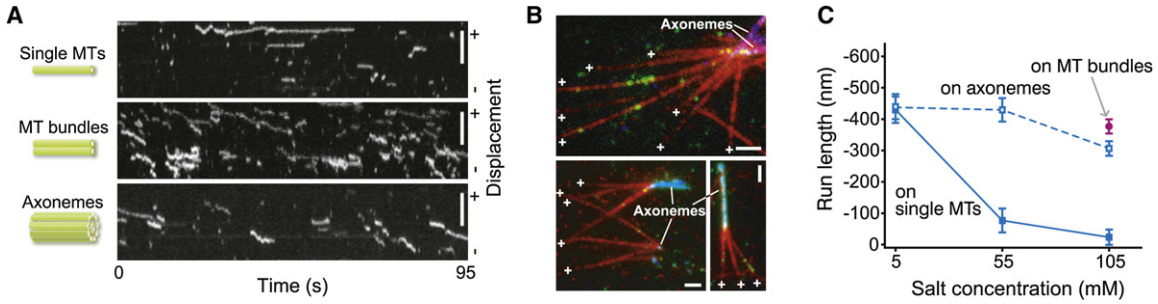

Figure 3. Effects of Ionic Strength and MT Bundling on Motility

(A) Kymographs showing the motion of GFP-Ncd195 in assay buffer containing 1 mM ATP and 105 mM KAc. Plus (+) and minus (−) symbols on the right refer to the polarity of the MT. Scale bars represent 3 μm.

(B) Typical TIRF images of bundled MTs grown from axonemes. The image of the Cy5-MTs (red) and GFP-Ncd (green) were overlaid on the image of the BODIPY FL-axonemes (blue). GFP-Ncd molecules on axonemes in the upper panel were photobleached after long exposure. Plus (+) symbols refer to the polarity of the MTs. Scale bars represent 2 μm.

(C) Run lengths of GFP-Ncd195 on single MTs, bundled MTs, and axonemes as a function of salt concentration. Each plot represents the mean ± SEM.

containing only the neck and motor domains) as well as GFP-Ncd195 and GFP-Ncd222 exhibited nonbiased one-dimensional diffusion along MTs, whereas kinesin-GFP did not move (Figure S6 and Table S2). GFP-Ncd333, a monomer construct, only showed association-dissociation events in short periods, almost within one frame (data not shown). These results suggest that dimeric Ncd head domains alone can diffuse along MTs in the weak binding state. Table S2 also shows that the K-rich region further supports the association with MTs by interacting with the E-hook.

MT Bundling Enhances the Processive Movement of GFP-Ncd195

Adding 50 mM KAc to the assay buffer virtually inhibited the unidirectional movement of GFP-Ncd195 along single MTs. Unexpectedly, we found that GFP-Ncd195 moved along bundled MTs even at 105 mM KAc (Figures 3A and 3C). The processive movement was observed when MTs were premixed with GFP-Ncd195 to form MT bundles. This processivity, even when electrostatic interactions were weakened at 105 mM KAc, could be explained by an increased interaction with the E-hooks of bundled MTs. To evaluate this hypothesis, we developed an assaying system specifically designed for monitoring the movement of single molecules on parallel MT bundles in which MTs are grown from an axoneme (Figure 3B). The axonemes define the polarity of the MTs that grow preferentially from the plus end of the axonemes and provide a rigid anchor for the MT bundles. We first confirmed that GFP-Ncd195 formed a dimer on MT bundles by measuring the fluorescence intensity (Figure S4). The bulk of GFP spots moved processively toward the axoneme, even at 105 mM KAc (Figure 3, Table 2, and Movie S2). We also used axonemes themselves as a more stable "rail" for the motility assay because they have doublet MTs that could mimic parallel MT bundles. GFP-Ncd moved processively along axonemes even at 105 mM KAc (Movie S3), as observed along MT bundles. MT bundling increases the number of E-hooks available for the tethering interaction and may prevent the complete dissociation of Ncd from MTs and allow effective rebinding to MTs (Figure 4B). These results indicate that GFP-Ncd195 can move processively, at least along parallel MT bundles. Because the tail region of Ncd interacts electrostatically with the MT, it would be plausible to expect that Ncd could move along "antiparallel" MT bundles that also are seen in mitotic spindles. However, further work is required to address this issue.

In this report, we provide the first evidence of a processive movement exhibited by individual minus-end-directed kinesins by using a single-molecule imaging technique. Our results

Table 2. Effects of Ionic Strength and Microtubule Bundling on Motility

		GFP-Ncd195					Kinesin-GFP				
MT Organization	KAc (mM)	Velocity (nm/s)	Run Length (nm)	Duration (s)	Diffusion Coefficient ($\times 10^4$ nm^2/s)	n	Velocity (nm/s)	Run Length (nm)	Duration (s)	Diffusion Coefficient ($\times 10^4$ nm^2/s)	n
Single MTs											
	5	−97 ± 4	−430 ± 40	3.4 ± 0.6	2.0 ± 0.3	230	690 ± 5	1620 ± 19	2.8 ± 0.1	0.48 ± 0.08	109
	55	−1.5 ± 0.3	−77 ± 36	2.1 ± 0.1	0.36 ± 0.09	79	760 ± 47	1320 ± 7	2.0 ± 0.1	0.61 ± 0.21	82
	105	−13 ± 7	−22 ± 26	1.4 ± 0.1	0.84 ± 1.20	81	800 ± 29	1370 ± 19	2.1 ± 0.1	0.99 ± 0.26	45
MT Bundles											
	105	−84 ± 5	−380 ± 22	2.9 ± 0.1	0.42 ± 0.06	209	ND	ND	ND	ND	
Axonemes											
	5	−65 ± 4	−440 ± 38	5.6 ± 0.1	0.81 ± 0.13	108	640 ± 4	1960 ± 30	2.6 ± 0.1	0.37 ± 0.08	45
	55	−74 ± 2	−430 ± 35	4.1 ± 0.1	0.84 ± 0.13	111	ND	ND	ND	ND	
	105	−91 ± 4	−310 ± 22	2.5 ± 0.1	1.4 ± 0.3	201	ND	ND	ND	ND	

Errors are given as the standard error of the fitted parameter except for the standard errors of run length of GFP-Ncd that were calculated from the raw data.
ND, not determined.

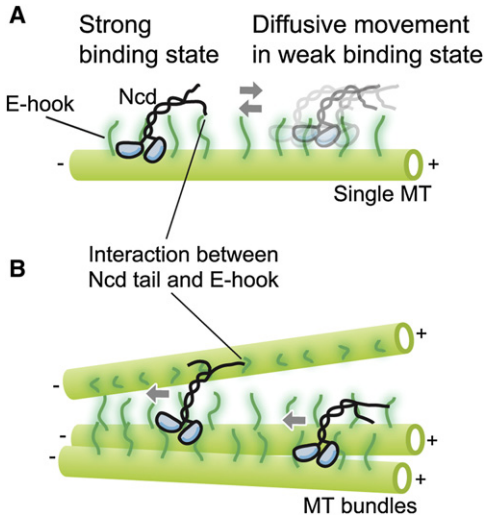

Figure 4. Model of Processive Movement of Ncd

(A) Schematic drawings of Ncd moving on a single microtubule (not to scale). In the strong binding state, Ncd binds rigidly to the MT, but in the weak binding state, it can move diffusively without detaching from the MT. The directional bias could be made by a "power stroke" or biased affinity toward the minus end of the MT while being tethered to it. The E-hooks are drawn for only one protofilament for simplicity.

(B) Processive movement of Ncd enhanced by MT bundling.

reveal that Ncd exhibited a distinct processivity from dimeric kinesin-1, containing a diffusive element that does not require ATP hydrolysis (Figure 4A). Such weak processivity also has been reported for KIF1A [18], Eg5 [20], and monomeric kinesin-1 [17]. The Ncd tail serves as a tether to MTs and thereby enables Ncd to behave as a processive motor, although the coupling between the steps and the ATP turnover would be looser compared with dimeric kinesin-1. However, even in dimeric kinesin-1, electrostatic interaction is reported to be important for processivity [21]. The electrostatic tethering mechanism might therefore be a general principle for processivity in both vesicle transporters and spindle motors.

Why, then, is Ncd not highly processive like the vesicle transporter kinesin-1? We found that individual GFP-Ncd molecules can modulate its processivity depending on MT bundling (Figure 4B). A recent study revealed that the turnover rate of Ncd on MT bundles is considerably high in vivo [10], suggesting that Ncd is a dynamic, not a static, crosslinker. Our results may reinforce this emerging view and provide further understanding of spindle formation. We speculate that the variable processivity of Ncd may reflect the physiological needs to dynamically assemble the spindle structure. The diffusive nature of Ncd in the weak binding state may allow Ncd to wait on single MTs without consuming ATP. When the MTs begin to be organized, Ncd would move with enhanced processivity along bundled MTs toward the minus end, forming transient crosslinks and sliding MTs. In this model, Ncd and the MTs form a feedback loop, namely by which more Ncd molecules would be activated by increasing numbers of bundled MTs, because the MT bundle is a product of crosslinking by Ncd itself. However, it remains unclear how Ncd molecules exert the force required to slide MTs. Previous studies have shown that self-organization of MT asters requires processive motors [28, 29], but individual dimeric Ncd molecules cannot step processively against the load [30]. The discrepancy could be resolved if small numbers of Ncd molecules acted cooperatively to generate the required force, as previously reported [16, 29, 31, 32]. The processivity of individual Ncd molecules at the low loads that we have shown here may be advantageous for efficient accumulation of Ncd and may lead to cooperative force generation in the ensemble by increasing local Ncd concentration. The variable processivity may be tuned such that crosslinks neither become too static nor too dynamic to efficiently assemble/disassemble the spindle. Further study on the cooperative behavior of spindle motors is needed to elucidate the underlying mechanisms.

Supplemental Data

Experimental Procedures, seven figures, two tables, and three movies are available at http://www.current-biology.com/cgi/content/full/18/2/152/DC1/.

Acknowledgments

This work was supported by a grant-in-aid for scientific research (B) from the Japan Society for the Promotion of Science (JSPS); a grant-in-aid for scientific research on priority areas from the Ministry of Education, Culture, Sports, Science, and Technology (MEXT); a Core Research for Evolutional Science and Technology (CREST) program grant from the Japan Science and Technology Agency (JST); and a grant-in-aid for JSPS fellows from JSPS.

Received: November 9, 2007
Revised: December 14, 2007
Accepted: December 19, 2007
Published online: January 17, 2008

References

1. Endow, S.A., Henikoff, S., and Soler-Niedziela, L. (1990). Mediation of meiotic and early mitotic chromosome segregation in Drosophila by a protein related to kinesin. Nature *345*, 81–83.
2. McDonald, H.B., Stewart, R.J., and Goldstein, L.S. (1990). The kinesin-like ncd protein of Drosophila is a minus end-directed microtubule motor. Cell *63*, 1159–1165.
3. Hatsumi, M., and Endow, S.A. (1992). The Drosophila ncd microtubule motor protein is spindle-associated in meiotic and mitotic cells. J. Cell Sci. *103*, 1013–1020.
4. Matthies, H.J., McDonald, H.B., Goldstein, L.S., and Theurkauf, W.E. (1996). Anastral meiotic spindle morphogenesis: role of the non-claret disjunctional kinesin-like protein. J. Cell Biol. *134*, 455–464.
5. Endow, S.A., and Komma, D.J. (1997). Spindle dynamics during meiosis in Drosophila oocytes. J. Cell Biol. *137*, 1321–1336.
6. Endow, S.A., and Waligora, K.W. (1998). Determinants of kinesin motor polarity. Science *281*, 1200–1202.
7. Foster, K.A., Mackey, A.T., and Gilbert, S.P. (2001). A mechanistic model for Ncd directionality. J. Biol. Chem. *276*, 19259–19266.
8. Chandra, R., Salmon, E.D., Erickson, H.P., Lockhart, A., and Endow, S.A. (1993). Structural and functional domains of the Drosophila ncd microtubule motor protein. J. Biol. Chem. *268*, 9005–9013.
9. Karabay, A., and Walker, R.A. (1999). Identification of microtubule binding sites in the Ncd tail domain. Biochemistry *38*, 1838–1849.
10. Goshima, G., Nedelec, F., and Vale, R.D. (2005). Mechanisms for focusing mitotic spindle poles by minus end-directed motor proteins. J. Cell Biol. *171*, 229–240.
11. Tao, L., Mogilner, A., Civelekoglu-Scholey, G., Wollman, R., Evans, J., Stahlberg, H., and Scholey, J.M. (2006). A homotetrameric kinesin-5, KLP61F, bundles microtubules and antagonizes Ncd in motility assays. Curr. Biol. *16*, 2293–2302.
12. Oladipo, A., Cowan, A., and Rodionov, V. (2007). Microtubule motor Ncd induces sliding of microtubules in vivo. Mol. Biol. Cell *18*, 3601–3606.
13. Case, R.B., Pierce, D.W., Hom-Booher, N., Hart, C.L., and Vale, R.D. (1997). The directional preference of kinesin motors is specified by an element outside of the motor catalytic domain. Cell *90*, 959–966.
14. Crevel, I.M., Lockhart, A., and Cross, R.A. (1997). Kinetic evidence for low chemical processivity in ncd and Eg5. J. Mol. Biol. *273*, 160–170.

15. Stewart, R.J., Semerjian, J., and Schmidt, C.F. (1998). Highly processive motility is not a general feature of the kinesins. Eur. Biophys. J. *27*, 353–360.
16. deCastro, M.J., Ho, C.H., and Stewart, R.J. (1999). Motility of dimeric ncd on a metal-chelating surfactant: evidence that ncd is not processive. Biochemistry *38*, 5076–5081.
17. Inoue, Y., Iwane, A.H., Miyai, T., Muto, E., and Yanagida, T. (2001). Motility of single one-headed kinesin molecules along microtubules. Biophys. J. *81*, 2838–2850.
18. Okada, Y., and Hirokawa, N. (1999). A processive single-headed motor: Kinesin superfamily protein KIF1A. Science *283*, 1152–1157.
19. Svoboda, K., Mitra, P.P., and Block, S.M. (1994). Fluctuation analysis of motor protein movement and single enzyme kinetics. Proc. Natl. Acad. Sci. USA *91*, 11782–11786.
20. Kwok, B.H., Kapitein, L.C., Kim, J.H., Peterman, E.J., Schmidt, C.F., and Kapoor, T.M. (2006). Allosteric inhibition of kinesin-5 modulates its processive directional motility. Nat. Chem. Biol. *2*, 480–485.
21. Thorn, K.S., Ubersax, J.A., and Vale, R.D. (2000). Engineering the processive run length of the kinesin motor. J. Cell Biol. *151*, 1093–1100.
22. Skiniotis, G., Cochran, J.C., Muller, J., Mandelkow, E., Gilbert, S.P., and Hoenger, A. (2004). Modulation of kinesin binding by the C-termini of tubulin. EMBO J. *23*, 989–999.
23. Lakamper, S., and Meyhofer, E. (2005). The E-hook of tubulin interacts with kinesin's head to increase processivity and speed. Biophys. J. *89*, 3223–3234.
24. Ito, M., Morii, H., Shimizu, T., and Tanokura, M. (2006). Coiled coil in the stalk region of ncd motor protein is nonlocally sustained. Biochemistry *45*, 3315–3324.
25. Makino, T., Morii, H., Shimizu, T., Arisaka, F., Kato, Y., Nagata, K., and Tanokura, M. (2007). Reversible and irreversible coiled coils in the stalk domain of ncd motor protein. Biochemistry *46*, 9523–9532.
26. Pechatnikova, E., and Taylor, E.W. (1997). Kinetic mechanism of monomeric non-claret disjunctional protein (Ncd) ATPase. J. Biol. Chem. *272*, 30735–30740.
27. Pechatnikova, E., and Taylor, E.W. (1999). Kinetics processivity and the direction of motion of Ncd. Biophys. J. *77*, 1003–1016.
28. Nedelec, F.J., Surrey, T., Maggs, A.C., and Leibler, S. (1997). Self-organization of microtubules and motors. Nature *389*, 305–308.
29. Surrey, T., Nedelec, F., Leibler, S., and Karsenti, E. (2001). Physical properties determining self-organization of motors and microtubules. Science *292*, 1167–1171.
30. deCastro, M.J., Fondecave, R.M., Clarke, L.A., Schmidt, C.F., and Stewart, R.J. (2000). Working strokes by single molecules of the kinesin-related microtubule motor ncd. Nat. Cell Biol. *2*, 724–729.
31. Badoual, M., Julicher, F., and Prost, J. (2002). Bidirectional cooperative motion of molecular motors. Proc. Natl. Acad. Sci. USA *99*, 6696–6701.
32. Sciambi, C.J., Komma, D.J., Skold, H.N., Hirose, K., and Endow, S.A. (2005). A bidirectional kinesin motor in live Drosophila embryos. Traffic *6*, 1036–1046.